JOURNAL OF APPLIED ELECTROCHEMISTRY **28** (1998) 899–905

Electrochemical impedance spectroscopic study of dimensionally stable anode corrosion

V. A. ALVES[1,2], L. A. da SILVA[2] and J. F.C. BOODTS[2,3]

[1] *Instituto de Química de São Carlos/USP, Av. Dr. Carlos Botelho, 1465 Caixa Postal 780 CEP 13560-970, São Carlos, SP, Brasil*

[2] *Departamento de Química da FFCLRP/USP, Av. Bandeirantes, 3900 CEP 14040-901, Ribeirão Preto, SP, Brasil*

[3] *Departamento de Química/Universidade Federal de Uberlândia Av. João Naves de Ávila, S/N CEP 38400-902, Uberlândia, MG, Brasil*

Received 10 July 1997; revised 20 October 1997

An electrode of nominal composition $Ti/Ir_{0.3}Ti_{0.7}O_2$ was prepared by thermal decomposition of the chloride precursor mixture at 450 °C. A systematic study of the corrosion behaviour of this anode was performed under accelerated conditions ($j = 400\,mA\,cm^{-2}$) in acidic media. Simultaneously, CV and EIS measurements were done at regular time intervals until the end of the electrode service life (~528 h). It was possible to identify the various stages of the electrode deactivation, and quantify the associated parameters. Three main steps were identified in the electrode deactivation mechanism. During the first 170 h, the loss of the more external (porous) part of the oxide active layer occurred. This is supported by the decrease in the parameter-values related to the electrochemically active surface area of the anode (q_a and C_{dl}) and an increase in the R_{ct}-values. The second stage is evidenced by a potential step afterwards remaining practically constant up to ~380 h, suggesting that the more compact and still very active region of the electrode is now exposed. Finally, for $t_{cor} > 400$ h the anode potential increases again. This behaviour, together with the R_{ct} against time, suggests that the most internal part of the original coating, less rich in IrO_2, is now exposed to the solution and is corroded. For $t \geq \sim 510$ h the anode potential increases rapidly, the electrode being totally deactivated at $t \simeq 528$ h, when the anodically grown TiO_2 film is exposed to the solution. During the complete deactivation process, the growth of a TiO_2 film, due to Ti-support oxidation, in addition to that already present (IrO_2 doped TiO_2 film formed during the calcination step), is evidenced by the increase in the R_f-values, as well as decreasing C_f-values. However, for $t_{cor} < 450$ h the rate of this process is not significant. Only for $t_{cor} > 450$ h Ti-support oxidation becomes the main feature of the deactivation process.

Keywords: *electrocatalysis*, *dimensionally stable anodes*, *mixed oxides*, *corrosion*, *impedance*

1. Introduction

Dimensionally stable anodes (DSAs®) are widely employed in the electrochemical industry. TiO_2 stabilized conductive metallic oxides, for example, RuO_2, IrO_2, used as a catalyst supported on Ti^o, result in an electrode with excellent catalytic and mechanical properties showing long service life under industrial conditions. The good mechanical properties, permitting lower anode/cathode gap, results in significant energy savings when compared to the older cells not using DSA® technology. Presently, DSAs® are increasingly used in the field of oxygen evolution. For technological applications the service life of any electrode material is always one of the main concerns. Normally, the service life of an electrode is determined under conditions of accelerated corrosion, imposing a high constant current to the system and measuring the potential against time response [1].

Electrochemical impedance spectroscopy (EIS) is a powerful technique which has been used to evaluate the electrochemical behaviour of a variety of materials. However, due to the particularities of the conductive metallic oxides little work has been done in the field of DSAs® [2–8].

To study the potential of EIS as a tool for following the corrosion behaviour of DSAs® an investigation of these electrode materials, under conditions of accelerated corrosion, was conducted using a Ti-supported IrO_2/TiO_2 mixture ($Ti/Ir_{0.3}Ti_{0.7}O_2$) as model system.

2. Experimental details

2.1. *Electrode preparation*

An electrode of nominal compositioin $Ti/Ir_{0.3}Ti_{0.7}O_2$ was prepared by thermal decomposition (450 °C) of

0021-891X

about 0.14 mol dm^{-3} solutions of $IrCl_3.xHCl.xH_2O$ (Aldrich) and $TiCl_4$ (Ventron) in 1:1 (v/v) HCl (Merck). The mixture of the precursor solutions of the desired mole ratio was spread onto both sides of the Ti support (10 mm × 10 mm × 0.15 mm) by brushing. The sandblasted support was etched in boiling 10% oxalic acid, for 10 min, just prior to depositing the oxide layer. After each application, the solvent was evaporated at about 80–90 °C and the dried layer fired for 5 min, under a 5 L min^{-1} oxygen stream, in a preheated oven. The operation was repeated until the desired oxide loading (1.3 mg cm^{-2}, corresponding to a nominal thickness of about 2 μm) was reached. The electrode was finally annealed at the same temperature for 1 h. On average four layers were necessary to reach the required oxide mass. The assembly of the electrodes and the special Teflon holder have been described elsewhere [9].

2.2. *Solution*

1.0 mol dm^{-3} $HClO_4$ (Merck) solution was used as supporting electrolyte. Experiments were conducted at 32 ± 2 °C.

2.3. *Techniques and instrumentation*

Surface characterization and monitoring during the corrosion study were done by recording cyclic voltammograms at 20 mV s^{-1}, over the 0.4–1.4 V vs RHE range, from 1.0 mol dm^{-3} $HClO_4$. The corrosion behaviour was investigated by submitting the electrode to a constant nominal current density, j, of 400 mA cm^{-2} and the E/t curve was recorded simultaneously. The service life (SL) of the electrodes was taken as the time necessary for complete deactivation of the electrode material (E = 6 V vs RHE). This time corresponded to ~528 h.

Impedance spectra, obtained at regular time intervals and constant d.c. potentials (1.48, 1.50 V vs RHE) covered the 5 mHz–100 kHz frequency interval. The morphological properties and the chemical composition of the electrode surface, before and after corrosion, were analysed by SEM and EDX.

Electrochemical measurements were carried out using a PAR (model 273A) potentiostat, monitored by a IBM (model 55/SX) personal computer. In the case of the impedance measurements, a PAR (model 5210) lock-in amplifier was also used. SEM and EDX analyses were done with a Zeiss (DSM 960) microscope equipped with a Link Analytical (QX 2000) X-ray energy microanalyser. A 20 keV electron beam was used.

3. Results and discussion

3.1. *Chronopotentiometric and voltammetric behaviour as a function of corrosion time*

The potential against time curve, obtained as a response to the constant nominal current, j, of 400 mA cm^{-2} applied to the $Ti/Ir_{0.3}Ti_{0.7}O_2$ electrode, is shown in Fig. 1. Based on the potential changes, three characteristic regions can be identified. After a constant potential region, a first increase in potential is observed at $t \simeq 170$ h, followed by a region where E is again constant. At $t \simeq 380$ h the potential approaches a new plateau. For $t > 450$ h the potential increases almost exponentially showing an abrupt increase at ~510 h when a total destruction of the catalytic properties is observed.

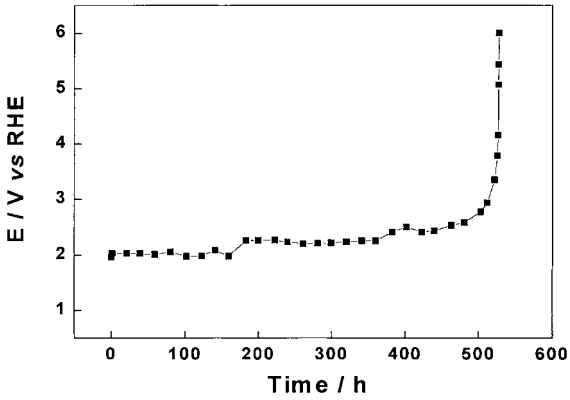

Fig. 1. E/t behaviour. j = 400 mA cm^{-2}. Supporting electrolyte: 1.0 mol dm^{-3} $HClO_4$. T = 32 ± 2 °C.

The first potential increase, after the initial constant potential region (0–170 h), reveals a slight decrease in the catalytic efficiency of the system and is attributed to the elimination of the more external and porous part of the active layer. This interpretation is consistent with SEM micrographs (showing the porous structure) and the well-known tendency of IrO_2 to segregate from oxide mixtures [10, 11]. The loss of the porous part of the oxide layer, attributed to a combination of erosion and corrosion, and the consequent decrease in roughness of the layer now exposed to the solution, results in a higher effective current density being sensed by the electrode, explaining the increase in the potential at ~170 h. The decrease in the electrochemical active surface area is supported by the anodic voltammetric charge, q_a/t curve which shows a decrease in q_a in the 150–180 h region (Fig. 2).

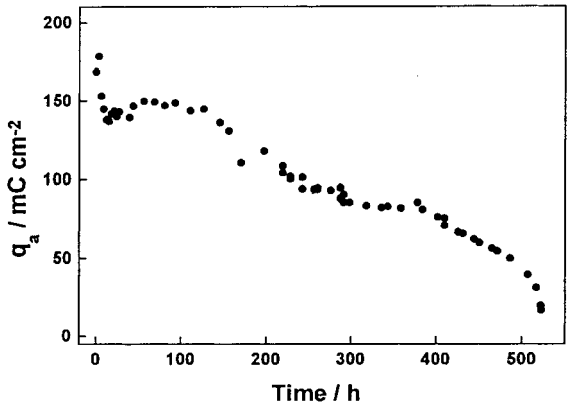

Fig. 2. Anodic voltammetric charge, q_a, as a function of corrosion time. Supporting electrolyte: 1.0 mol dm^{-3} $HClO_4$. v = 20 mV s^{-1}. q_a obtained integrating the i/E curve over the 0.4–1.4 V vs RHE interval.

The second region (180–370 h) in the E/t curve can be attributed to slow corrosion of the more compact part of the active layer which still possesses excellent catalytic activity. The slow corrosion of this part of the active oxide layer is consistent with the low rate of change in the q_a/t curve in the same region.

In the third region of the E/t curve the rate of increase in potential changes significantly while the q_a/t curve shows a simultaneous decrease in exposed surface area. This behaviour suggests that the quantity of catalytic material available can no longer sustain the lower potentials observed in the earlier stages. For $t > 500$ h both E and q_a/t show a sudden change, corresponding to the beginning of anode deactivation, due to the consumption of the oxide layer and passivation through the anodically grown TiO_2 interlayer. After deactivation q_a represents about 11% of the original charge (Fig. 3), showing that a small quantity of catalytic material is still present.

Compared to RuO_2, IrO_2 has better resistance to anodic corrosion. However, at $E \geq 2.0$ V vs RHE its corrosion rate becomes significant due to the formation of soluble IrO_4^{2-} species [12]. Thus, for $t < 170$ h material loss is probably caused by a combination of corrosion and erosion, the latter being due to the strong oxygen evolution. For $t > 170$ h the main process is corrosion since for these stages the electrode potential is more anodic (favoring corrosion) while a more compact layer is exposed to the solution (less erosion).

3.2. *Electrochemical impedance spectroscopy (EIS)*

Initially, the impedance spectrum in the complex plane ($-Z_{imag}/Z_{real}$) at low frequencies shows a well formed semicircle related to the OER, while at high frequencies the beginning of a small semicircle is observed, which is related to the oxide film properties [2–4, 12, 13]. The impedance behaviour at high frequencies is attributed to the IrO_2-doped TiO_2 film, formed during the calcination step at the Ti^o-support surface. In fact, the structure of the Ti^o/oxide layer interface, Ti^o/OL, can be considered as a capacitor made-up of Ti^o-support/IrO_2-doped TiO_2 (the dielectric)/oxide mixture (a metallic conductor) (see Fig. 4(a)).

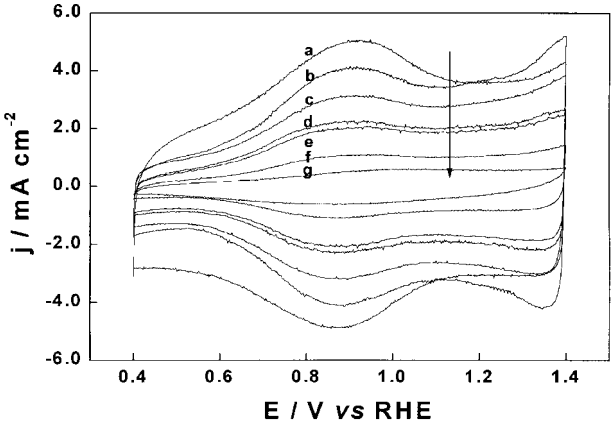

Fig. 3. Cyclic voltammograms as a function of corrosion time, t_{cor}: (a) 0, (b) 93, (c) 197, (d) 323, (e) 407, (f) 512 and (g) 528 h. Supporting electrolyte: 1.0 mol dm^{-3} $HClO_4$. $v = 20$ mV s^{-1}.

The formation of this film is supported by X-ray diffraction analyses [14], which showed the presence of TiO_2, in the anatase and rutile forms, and Ti_2O_3 diffraction peaks in a freshly prepared film of nominal composition $Ti/Ir_{0.3}Ce_{0.7}O_2$, which does not contain titanium oxide as a component. As shown in Fig. 5, the small semicircle at high frequencies becomes much better defined with increasing corrosion time, t_{cor}.

Interestingly, in the final stages of the E/t curve ($t_{cor} > \sim 400$ h) a third semicircle starts forming in the high frequency domain, becoming a prominent feature of the impedance spectra (see Fig. 5, insets). The appearance of the third semicircle coincides with the time that all other parameters change drastically, suggesting a considerable loss of catalytic activity.

Using Boukamp's EQUIVCRT program [15], experimental data were fitted to a $R_\Omega(R_fQ_f)(R_{ct}Q_{dl})$ equivalent circuit (EC) where the f subscript refers to the properties of the film, the other symbols having their usual meaning. Since DSAs® normally show a high degree of roughness and inhomogeneities a constant phase element (CPE) instead of capacitance was used to fit the data [16–20].

From the CPE exponents (n values) it is possible to identify the physical significance of this element. The CPE of the semicircle related to the OER gives n-values close to 1, suggesting this element behaves as a capacitor, so: $Q_{dl} \equiv C_{dl}$. On the other hand, the n-values of the CPE related to the semicircle at high frequencies initially show values close to 0.6, at the end of the experiment, tending towards 0.8. These initial n values, although far from unity, refer to a capacitive element and can be attributed to heterogeneities of the oxide composition formed at the Ti support/oxide layer interface (see Fig. 4(a)). In fact, according to Martelli *et al.* [12], the structure of the oxide formed at this interface is extremely variable: amorphous or polycrystalline, anhydrous or hydrated films can be obtained, depending on the preparation procedure. Other possibilities are the formation of a nonstoichiometric $TiO_{(2-x)}$ [12], or even of a mixed $Ir_xTi_{(1-x)}O_2$ interlayer [13]. The increase in n-values can be explained in terms of the growth of a TiO_2 film due to support oxidation (Fig. 4(b) and (c)), which is corroborated by the increase in the R_f-values. Probably, the response of this non-Ir-doped TiO_2 film superposes on that of the film formed during the calcination step, providing higher n values. Another possibility is that the oxide film formed during the calcination step acquires a more stoichiometric structure. Close to the end of the service life the interlayer behaves as an almost perfect capacitive element, $n \simeq 0.9$, since at that moment the anodically grown TiO_2 (an almost ideal dielectric) controls the behaviour of the Ti/OL interface (see Figs 4(d) and 5).

The solution resistance values, R_Ω, as expected, remain practically constant between 0.7 and 1.2 Ω cm^2 during the whole experiment.

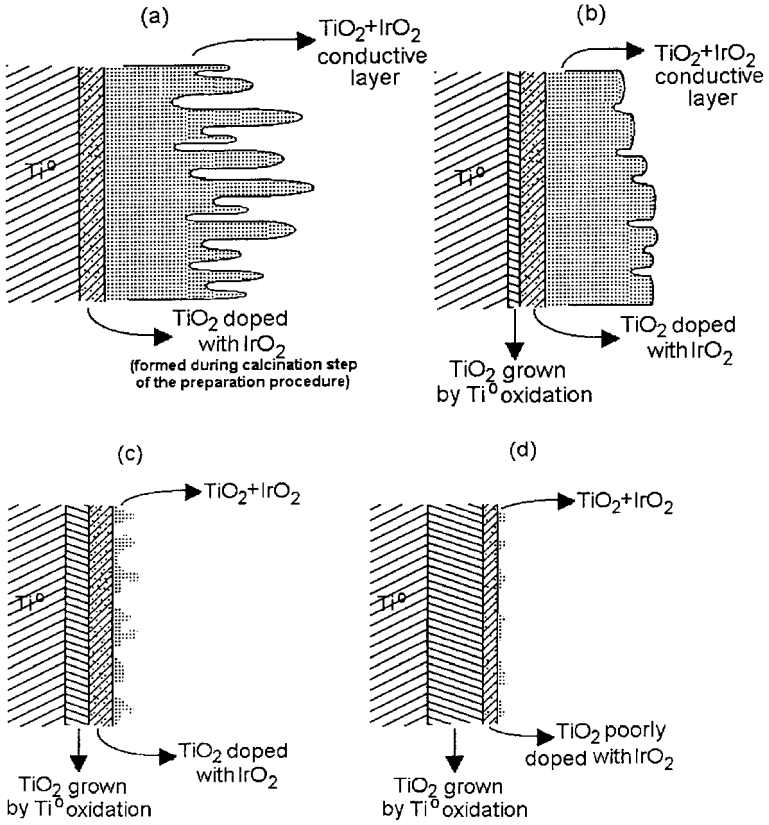

Fig. 4. Sketch of the electrode oxide structures during the various stages of the corrosion experiment. (a) New electrode; (b) electrode after elimination of the more porous part of the active layer; (c) electrode after loss of the conductive layer and (d) complete deactivation of the electrode SL.

As shown in Fig. 6, the film resistance values, R_f, after a few hours rapidly increase to $\sim 0.5\,\Omega\,cm^2$, staying almost constant until $t_{cor} \simeq 150\,h$. For $t_{cor} > 150\,h$, R_f increases steadily reaching a new limit of ~ 1.3–$1.4\,\Omega$ cm^2, at $t_{cor} \simeq 300\,h$ afterwards only increasing marginally until total deactivation of the electrode material, when R_f increases abruptly to $\sim 12\,\Omega$ cm^2. Thus, R_f can be identified with the resistance of the TiO_2 interlayer slowly growing through oxidation of the Ti-support (resulting in a TiO_2 film poorly doped with IrO_2) superposed on the response of the original IrO_2 doped TiO_2 interlayer (compare Fig. 4(a) and 4(b)). This interpretation is consistent with the film capacitance, C_f, as a function of time, which shows a rapid decrease in C_f from $\sim 80\,mF\,cm^{-2}$ to $\sim 9\,mF\,cm^{-2}$ until $\sim 200\,h$, only slightly decreasing for $t_{cor} > 200\,h$ (see Fig. 7).

The charge transfer resistance values, R_{ct}, stay constant during the initial 150 h, afterwards increasing until a new plateau is reached at $180\,h < t_{cor} < 300\,h$. For $t_{cor} > 300\,h$ R_{ct} steadily increases up to complete loss of the electrocatalytic behaviour of the electrode, when a value of ~ 230–$330\,\Omega$ cm^2 is obtained. Interestingly, these changes in the R_{ct}-values coincide with the breaks in the E/t curve (Fig. 1) and reflect the loss of IrO_2, resulting in a decrease of catalytic activity at a particular stage of the experiment, for example, the sudden increase in R_{ct} observed at $\sim 528\,h$ is consistent with the almost complete loss of the catalyst (TiO_2 is a bad catalyst for the OER). This behaviour is illustrated in Fig. 8.

The R_{ct}/t_{cor} behaviour is corroborated by both the double layer capacitance, C_{dl}, and anodic charge, q_a, as a function of time curves, which show changes in the respective parameters at exactly the same t_{cor} values (see Figs 9 and 2, respectively). The behaviour of C_{dl} as a function of t_{cor} is consistent with the proposed model (see Fig. 4). As can be seen from Fig. 9 the double layer capacitance is almost constant ($\sim 120\,mF\,cm^{-2}$) up to $\sim 180\,h$ when a sudden decrease, corresponding to the elimination of the more external rough part of the active layer, is observed. Then, C_{dl} stays constant at $\sim 60\,mF\,cm^{-2}$ during the 300–400 h interval when the more compact structure of the active layer is being corroded. At 528 h a sharp drop to $\sim 3\,mF\,cm^{-2}$ occurs when the electrode becomes deactivated and the anodically grown TiO_2-film at the Ti/OL interface, known to be compact, is exposed to the solution.

Tafel coefficients were calculated using Equation 1 [21, 22]:

$$b = 2.303\,R_{ct} i_{ss} \quad (1)$$

where i_{ss} is the steady state current measured immediately before each EIS analysis. Tafel coefficient behaviour as a function of t_{cor}, shown in Fig. 10, is consistent with R_{ct}, C_{dl} and q_a behaviour.

3.3. *Surface characterization of the oxide layer*

The morphology and chemical composition of the oxide layer was investigated by SEM and EDX before and after the corrosion experiment.

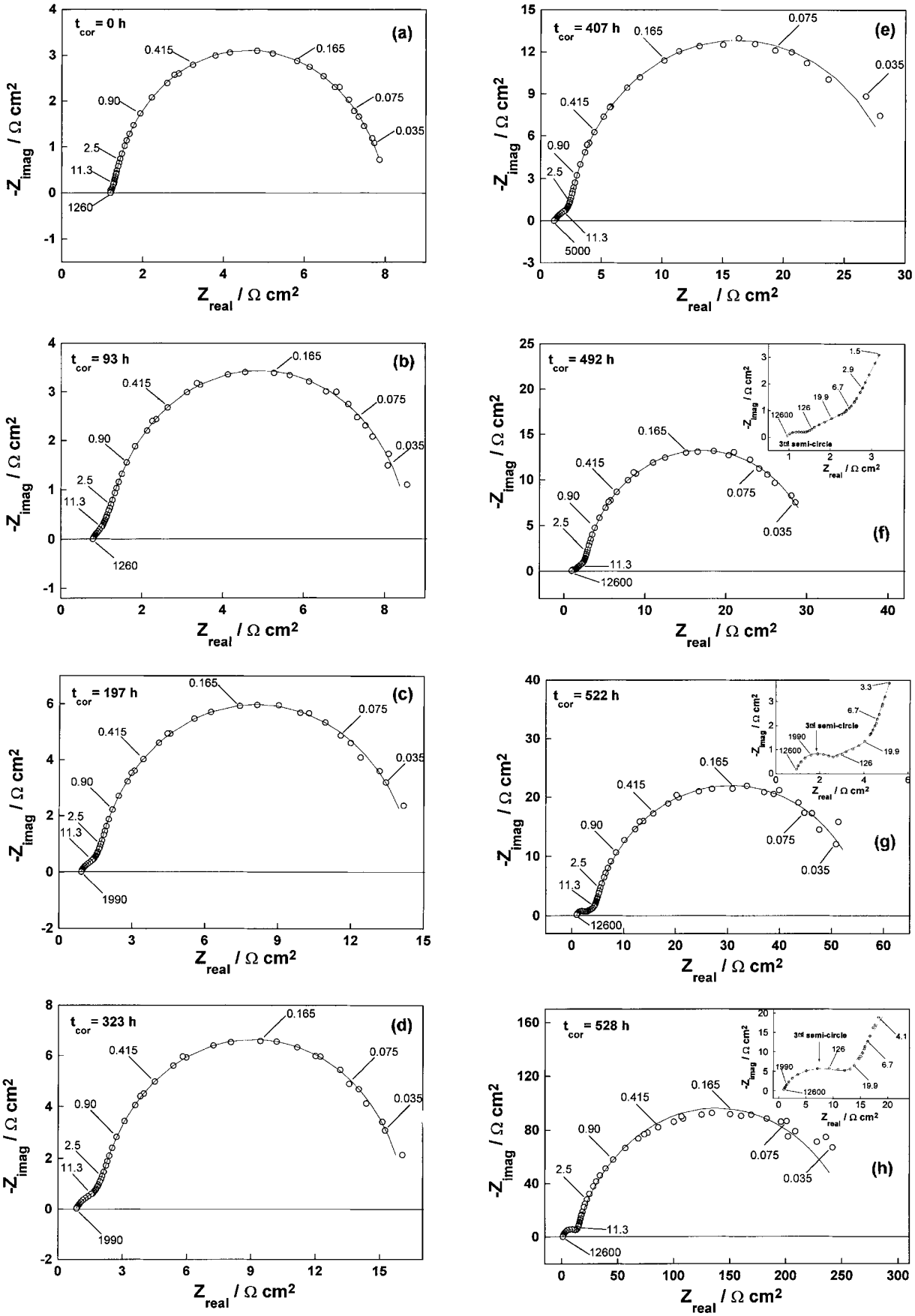

Fig. 5. Impedance spectra in the complex plane as a function of corrosion time. $E_{ap} = 1.50$ V vs RHE Key: (○) experimental data and (—) simulation. Numbers on curves are frequencies (in Hz). Insets show the high frequency part of the spectra.

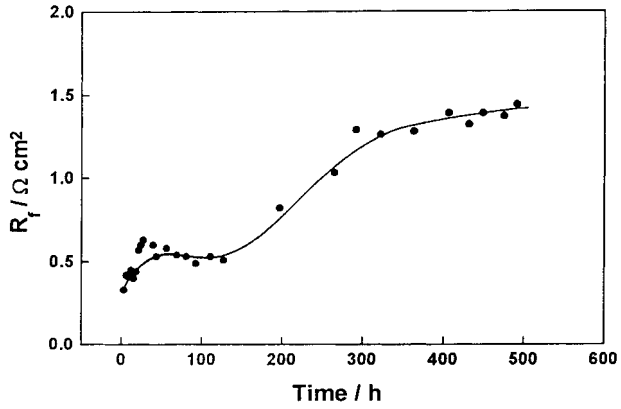

Fig. 6. Resistance, R_f, of the interlayer at the Ti/OL interface as a function of corrosion time. $E_{ap} = 1.50$ V vs RHE.

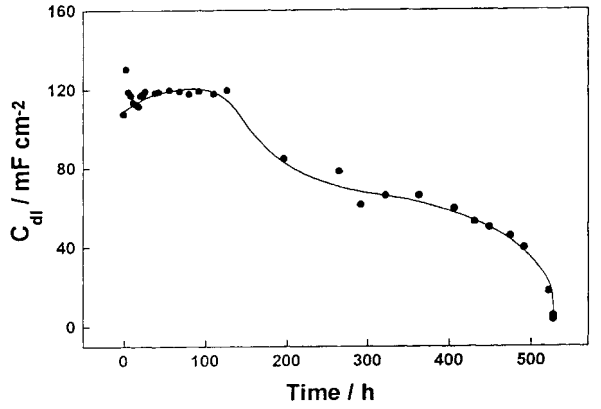

Fig. 9. Double layer capacitance, C_{dl}, as a function of corrosion time. $E_{ap} = 1.50$ V vs RHE.

The SEM micrograph of the freshly prepared oxide layer (Fig. 11(a)) shows the well-known cracked-mud structure, typical of high TiO_2 content conductive metallic oxide mixture [23]. The real composition of the oxide layer, obtained from quantitative EDX analysis, is different from the nominal. The Ir atomic percentage (19.3%) is lower than that expected from the nominal composition

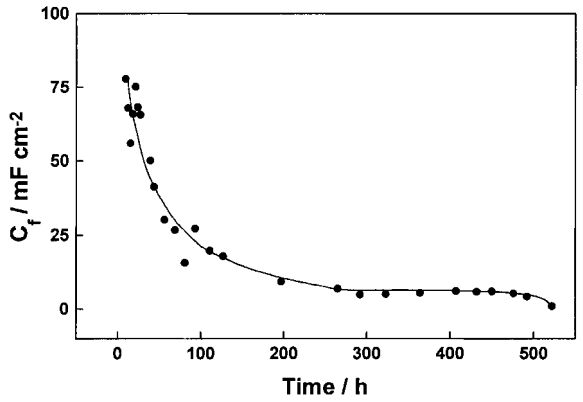

Fig. 7. Capacitance, C_f, of the interlayer Ti/OL as a function of corrosion time. $E_{ap} = 1.50$ V vs RHE.

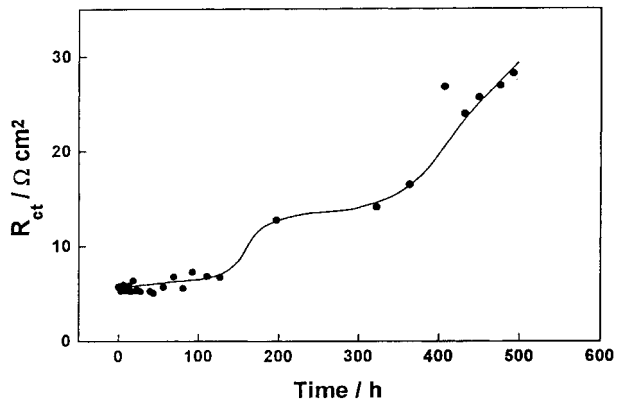

Fig. 8. Charge transfer resistance, R_{ct}, as a function of corrosion time. $E_{ap} = 1.50$ V vs RHE.

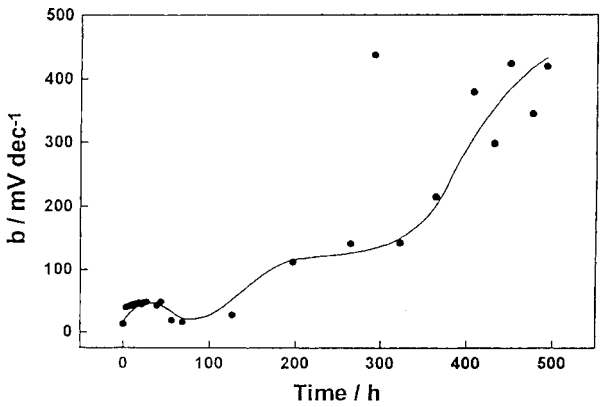

Fig. 10. Tafel coefficients, b, (obtained from Equation 1) as a function of corrosion time. $E_{ap} = 1.48$ V vs RHE.

(30%) and suggests TiO_2 enrichment of the layer, as also reported by other workers [24]. In our case this can be attributed to the high acidity (HCl 1:1 (v/v)) of the solvent used to dissolve the precusor salts, resulting in partial dissolution of the Ti-support being responsible for the high Ti atomic percentage (80.7%) found by EDX.

The SEM micrograph, obtained at the end of the corrosion study, reveals a totally different structure (see Fig. 11(b)). However, it is very similar to the structure observed by SEM for a preheated, bare, Ti-support [25]. EDX analysis shows Ir 2.80 at % when the electrode is deactivated. This small quantity of IrO_2 represents 14% of the initial content. This result is consistent with the anodic voltammetric charge, which also indicates the presence of IrO_2 at the end of the experiment and represents approximately 11% of the original voltammetric charge.

Acknowledgements

V. A. Alves and L. A. da Silva wish to acknowledge the FAPESP and CAPES foundations (Brazil), respectively, for a fellowship. J. F. C. Boodts acknowledges financial support received from FAPEMIG, PADCT II and CNPq.

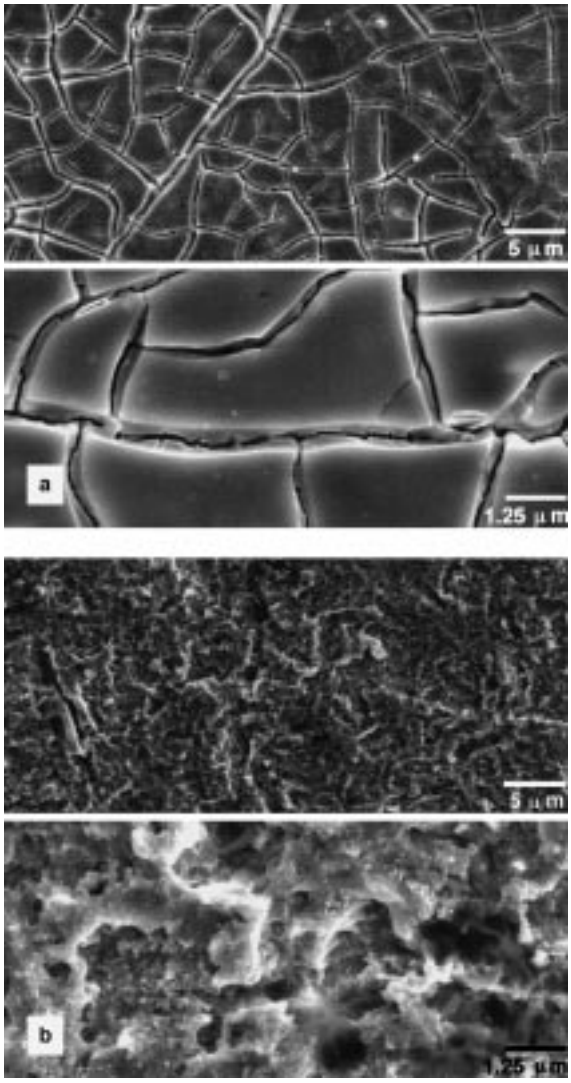

Fig. 11. SEM micrographs of freshly prepared electrode (a) and after corrosion investigation (b). Electrode nominal composition $Ti/Ir_{0.3}Ti_{0.7}O_2$.

References

[1] G. P. Vercesi, J. Rolewicz and Ch. Comninellis, *Thermochim. Acta* **176** (1991) 31.
[2] L. A. da Silva, V. A. Alves, M. A. P. da Silva, S. Trasatti and J. F. C. Boodts, *Electrochim. Acta* **41** (1996) 1279.
[3] *Idem, ibid.* **42** (1997) 271.
[4] *Idem, Can. J. Chem.* **75** (1997) 1483.
[5] D. T. Shieh and B. J. Hwang, *Electrochim. Acta* **38** (1993) 2239.
[6] L. Chen, D. Guay and A. Lasia, *J. Electrochem. Soc.* **143** (1996) 3576.
[7] I. R. Burrows, J. H. Entwistle and J. A. Harrison, *J. Electroanal. Chem.* **77** (1977) 21.
[8] I. R. Burrows, D. A. Denton and J. A. Harrison, *Electrochim. Acta* **23** (1978) 493.
[9] R. Garavaglia, C. M. Mari and S. Trasatti, *Surf. Technol.* **23** (1984) 41.
[10] V. A. Alves, L. A. da Silva, S. C. de Castro and J. F. C. Boodts, *J. Chem. Soc., Faraday Trans.* **94** (1998) 711.
[11] L. A. da Silva, V. A. Alves, S. Trasatti and J. F. C. Boodts, *J. Electroanal. Chem.* **427** (1997) 97.
[12] G. N. Martelli, R. Ornelas and G. Faita, *Electrochim. Acta* **39** (1994) 1551.
[13] F. Beck, *ibid.* **34** (1989) 811.
[14] V. A. Alves, L. A. da Silva and J. F. C. Boodts, 41st Brazilian Ceramic Meeting, 3–6 June 1997, São Paulo, Brazil. Extended Abstracts.
[15] B. A. Boukamp 'Equivalent Circuit', University of Twente, The Netherlands (1989).
[16] A. Lasia and A. Rami, *J. Electroanal. Chem.* **294** (1990) 123.
[17] Y. Choquette, A. Lasia, L. Brossard and H. Menard, *J. Electrochem. Soc.* **137** (1990) 1723.
[18] G. J. Brug, A. L. G. Van den Eeden, M. Sluyters-Rehbach and J. H. Sluyters, *J. Electroanal. Chem.* **176** (1984) 275.
[19] J. R. MacDonald, (Ed.), 'Impedance Spectroscopy' J. Wiley & Sons, New York (1987).
[20] R. D. Armstrong and M. Henderson, *J. Electroanal. Chem.* **39** (1971) 81.
[21] R. D. Armstrong, K. Edmondson and R. E. Firman, *ibid.* **40** (1972) 19.
[22] R. D. Armstrong and M. Henderson, *ibid.* **40** (1972) 121.
[23] K. Kameyama, K. Tsukada, K. Yahikozawa and Y. Takasu, *J. Electrochem. Soc.* **140** (1993) 966.
[24] J. Kristóf, J. Mink, A. De Battisti and J. Liszi, *Electrochim. Acta* **39** (1994) 1531.
[25] J. Krýsa, L. Kule, R. Mráz and I. Rousar, *J. Appl. Electrochem.* **26** (1996) 999.